

UIT - Secteur de la normalisation des télécommunications  
ITU - Telecommunication Standardization Sector  
UIT - Sector de Normalización de las Telecomunicaciones

**Study Period 1997-2000**

Commission d'études ;Study Group;Comisión de Estudio} **15**

Contribution tardive;Delayed Contribution ;Contribución tardía} **D.xxx**

Geneva, 21 June – 2 July, 1999

Texte disponible seulement en ;Text available only in;Texto disponible solamente en} **E**

Question(s): 4/15

SOURCE\*: IBM Europe

TITLE: Filtered Multitone Modulation

---

#### ABSTRACT

**This contribution describes the basic principles of filtered multitone (FMT) modulation and presents an analysis of the performance and complexity of this technique for VDSL transmission. FMT designates a form of polyphase filter-bank modulation where a high level of spectral containment is achieved for subchannel spectral shaping. It borrows features from CAP/QAM and DMT modulation techniques and offers advantages that go beyond those of each of these two modulation schemes taken individually.**

**The paper is tutorial in nature and does not aim at specifically addressing all VDSL system requirements. These aspects will be considered in a future contribution.**

---

\* **Contact:** Giovanni Cherubini (cbi@zurich.ibm.com) +41-1-724 85 18  
Evangelos Eleftheriou (ele@zurich.ibm.com) +41-1-724 85 83  
Sedat Ölçer (oel@zurich.ibm.com) +41-1-724 84 80

IBM Zurich Research Laboratory  
Säumerstrasse 4  
8803 Rüschlikon  
Switzerland

## 1. Introduction

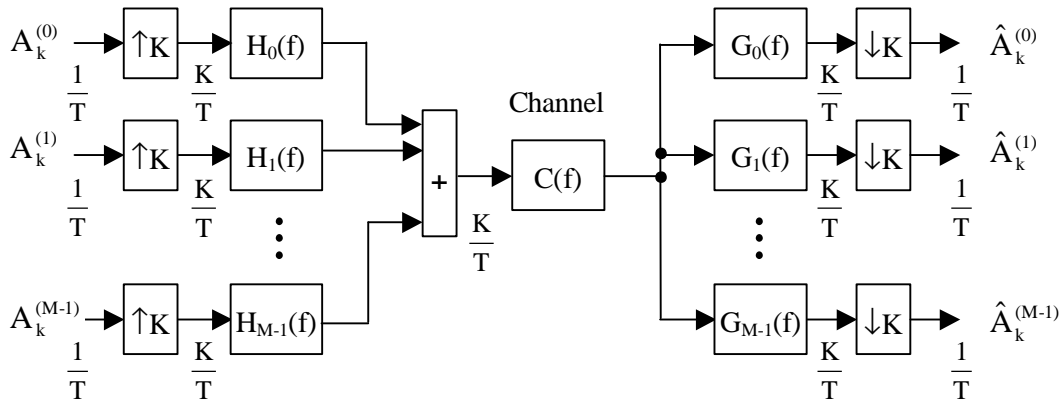
This contribution describes filtered multitone modulation (FMT) and its application to VDSL transmission. FMT modulation designates a form of polyphase filter-bank modulation technique where a high level of subchannel signal spectral containment is achieved by spectral shaping. The advantages of special subchannel spectral shaping will be shown in the context of a VDSL transmission system employing frequency division duplexing (FDD) where echo and crosstalk signals represent the main sources of disturbance.

In Section 2, we introduce some general concepts from the theory of filter-bank systems, which find their roots in multirate digital signal processing. In Section 3, we describe FMT modulation. Efficient realizations of transmit and receive filters that achieve a high level of subchannel spectral containment are discussed and several examples are introduced. In Sections 4 and 5, we identify the advantages of the described technique with respect to CAP/QAM and synchronous DMT modulations and investigate the performance of FMT-based transmission for a VDSL system employing FDD. Implementation complexity and system latency are two important implementation aspects that are addressed in Section 6. Finally, in Section 7, we provide some concluding remarks.

The purpose of this contribution is to present FMT modulation as a generic technology. Therefore an analysis that addresses all the system requirements set forth for VDSL within various standardization groups goes beyond the scope of the present study.

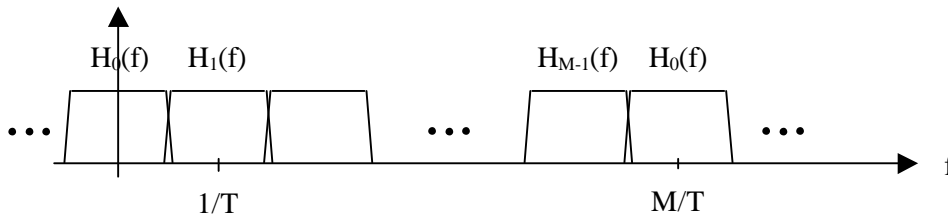
## 2. Filter-bank modulation

Figure 1 shows the block-diagram of a communication system employing filter-bank modulation and demodulation concepts. A group of  $M$  modulation symbols  $A_k^{(i)}$ ,  $i = 0, 1, \dots, M-1$ , is input in parallel at the rate of  $1/T$  into a set of  $M$  filters with transfer functions  $H_0(f)$ ,  $H_1(f)$ ,  $\dots$ ,  $H_{M-1}(f)$ . The notation  $\uparrow K$  indicates upsampling by a factor  $K$ , i.e., insertion of  $K-1$  zero signals between two consecutive input signals. This set of  $M$  filters represents a so-called *synthesis* filter-bank. The channel input signal is generated at the transmission rate of  $K/T$ . At the receiver, demodulation is achieved by an *analysis* filter bank that includes  $M$  filters  $G_0(f)$ ,  $G_1(f)$ ,  $\dots$ ,  $G_{M-1}(f)$  followed by downsamplers denoted by  $\downarrow K$ . When  $M = K$ , a *critically sampled* filter-bank structure is obtained.



**Figure 1:** General representation of a communication system using filter banks

Selection of filter characteristics plays a central role in the design of a communication system employing filter-bank modulation. The filters  $H_i(f)$  and  $G_i(f)$ ,  $i = 0, 1, \dots, M-1$ , typically exhibit a bandpass characteristic. Figure 2 shows an example of filter characteristics for a critically sampled filter bank where the  $i^{\text{th}}$  filter transfer function is centered on the frequency  $i/T$ . The necessity of oversampling each subchannel signal by a factor  $M$  can be immediately deduced from this figure since the spectral characteristic of each subchannel is periodic with period  $M/T$ .



**Figure 2:** Typical subchannel characteristics of a critically sampled  $M$ -band filter bank

In practice, filter-bank modulation systems are almost never implemented directly as shown in Figure 1. The reason for this is that, in this configuration, filters must operate at a rate that is  $K$  times faster than the symbol rate  $1/T$ . If the filters are appropriately selected, it is possible to achieve very efficient realizations. For example in the critically sampled case, if the  $M$  transmit [receive] filters are selected as the frequency-shifted versions of a baseband filter  $H(f)$  [ $G(f)$ ], the so-called *prototype filter*, the system of Figure 1 can be redrawn as shown in Figure 3(a), which in turn is equivalent, for the case  $M = K$  and assuming the matched filter pair condition<sup>1</sup>

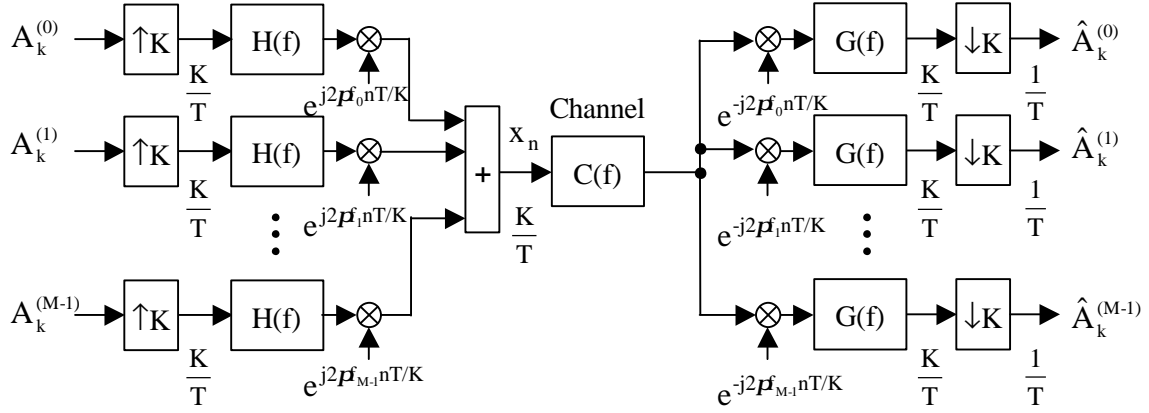
$$\mathbf{g}_n^{(i)} = \mathbf{h}_{-n}^{(i)*}, \quad i = 0, 1, \dots, M-1$$

is satisfied, to the system depicted in Figure 3(b), as shown in the Appendix [1]. The discrete-time modulations with the complex exponentials have been absorbed into the inverse discrete Fourier transformations (IDFTs) and the filtering operations on the  $M$  branches are performed by filters that correspond to the  $M$  *polyphase components* of the prototype filter. In other words, the  $H^{(i)}(f)$ ,  $i = 0, 1, \dots, M-1$ , represent the transfer functions of the  $M$  polyphase components of  $H(f)$ , and likewise at the receiver. This  $M$ -branch polyphase filter bank structure is attractive because the filtering operations are performed at the rate of  $1/T$  instead of  $M/T$ . It also has the advantage that only suitable prototype filters must be determined, not the complete set of analysis and synthesis filters. Efficient polyphase filter bank realizations can likewise be found in the noncritically sampled case. The decomposition of a filter characteristic into its polyphase components is explained in the Appendix.

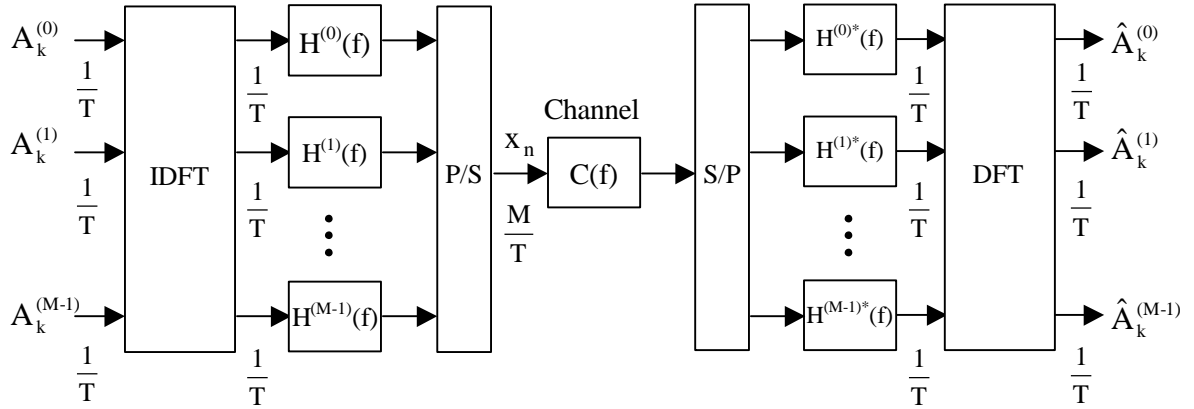
The reader will readily notice similarities between the structures shown in Figure 1 and 3 and those of CAP/QAM as well as DMT modulation systems. A passband single carrier system is obtained when only one branch  $i$  ( $i > 0$ ) of the filter bank in Figure 1 is retained. A DMT modulation system is obtained when all the polyphase filters in Figure 3(b) are reduced to unity gain.

Filter banks have been extensively studied in the area of discrete-time multirate signal processing [2]. In particular, filter bank structures for which the matched filter pair condition holds, have received considerable attention. In the vast majority of these applications, the following conditions are further imposed for the design of the filter bank:

<sup>1</sup> The asterisk denotes complex conjugation



(a) Filter bank modulation system employing baseband prototype filters



(b) Efficient implementation of the filter bank shown in (a) for  $M=K$

**Figure 3:** Efficient filter bank implementation using polyphase filter components

$$\sum_n h_n^{(i)} h_{n-k}^{(i)*} = \mathbf{d}_k, \quad i = 0, 1, \dots, M-1$$

$$\sum_n h_n^{(i)} h_{n-k}^{(j)*} = 0, \quad i \neq j.$$

For an ideal transmission channel that does not introduce signal distortion and noise, the above conditions guarantee “perfect reconstruction” for all the branches of the synthesis/analysis structure. This means that the symbols received at the output of each subchannel are free of interchannel as well as intersymbol interference, i.e.,

$$\hat{A}_k^{(i)} = A_k^{(i)}$$

up to a time delay introduced by the overall channel. In practice, perfect reconstruction requires that substantial spectral overlap of adjacent subchannels be allowed.

The above criterion appears to be meaningful for many applications, typically for subband coding of audio and video signals. Also in discrete wavelet multitone (DWMT) modulation [3], a technique that has been investigated for DSL transmission, the prototype filter is designed such that perfect reconstruction is possible at the demodulator output under the assumption of an ideal channel without noise and distortion.

The perfect reconstruction constraint may, however, be overly restrictive or even not suitable for filter design in a data communications context, because it enforces zero intersymbol and interchannel interference but ignores noise and distortion that are always present in practical communication channels. By relaxing the above constraints and introducing signal equalization capabilities at the receiver, prototype filters leading to better overall system performance and communications efficiency can be found.

### 3. Filtered multitone (FMT) modulation: general principles

We designate by filtered multitone (FMT) modulation a polyphase filter bank modulation technique where the prototype filter is designed to achieve a high level of subchannel spectral containment. In other terms, the prototype filter is designed such that at the output of each subchannel the level of interchannel interference may be considered negligible as compared to the level of other noise signals. In some cases, high spectral containment will be more easily achieved by relaxing the zero intersymbol constraint. In some other cases, our general polyphase filter-bank modulation approach will also enable alternative solutions to reach high spectral isolation between subchannels, as illustrated below. At the receiver of an FMT system, per-subchannel signal equalization is employed. According to the particular application and/or the desired system performance level, usually specified in terms of the mean-square error at the receiver decision point or of bit error probability, a symbol-spaced or fractionally-spaced linear equalizer can be used. Alternatively, symbol-spaced or fractionally-spaced decision-feedback equalization can be implemented, possibly in the form of precoding [4].

High level of subchannel spectral containment is a desirable property for many applications. For example, because leakage of signal energy between subchannels may be considered negligible, echo cancellation is not needed in frequency-division duplexing (FDD) transmission systems where subchannels are closely placed to each other. Also, in Zipper-like FDD [5], where all transmissions within the same cable binder adopt the same upstream/downstream frequency band allocations, self-NEXT is completely avoided. We note that known multicarrier modulation techniques lead to nonnegligible spectral overlap between the subchannels. For DMT modulation, the spectra of adjacent subchannels approximately “cross” at the  $-3$  dB point and the first sidelobe for a subchannel is as high as  $-13$  dB. For DWMT modulation, although the first sidelobe is as low as  $-45$  dB or less, the spectra of adjacent subchannels still cross at  $-3$  dB. Hence, a significant amount of subchannel signal energy couples into the neighboring subchannels.

For FMT modulation, the transmit polyphase filters are usually obtained from a linear-phase FIR prototype filter of length  $gM$ , i.e.,  $h_n = 0$  for  $k < 0$  and  $k \geq gM$ . Hence each of the  $M$  polyphase filter components has length  $g$ . In general, larger values of  $g$  allow better approximation of prototype filter transfer functions with sharp spectral roll-offs but lead to an increase in system latency. Clearly, the choice of the prototype filter allows various tradeoffs between number of subchannels, level of

spectral containment, signal latency and transmission efficiency. In this section, two examples will be treated to illustrate prototype filter selection.

As a first example, we consider a critically sampled FMT system that employs a prototype filter with frequency response providing a close approximation to the characteristic

$$\tilde{H}_1(f_N) = \begin{cases} \left| \frac{1 + e^{-j2\pi f_N}}{1 + r e^{-j2\pi f_N}} \right| & \text{if } |f_N| \leq 1/2 \\ 0 & \text{otherwise,} \end{cases}$$

where the parameter  $0 \leq r \leq 1$  controls the “roll-off” towards the spectral nulls at bandedge frequencies and  $f_N$  denotes frequency normalized by the symbol rate. This zero excess bandwidth characteristic leads to an FMT system ideally free of interchannel interference but with intersymbol interference within a subchannel. Figure 4 shows the subchannel characteristics that are obtained by using a prototype FIR filter that approximates the characteristic  $\tilde{H}_1(f)$  in the case where  $M = 256$ ,  $\uparrow = 10$ , and  $r = 0.1$ . For  $r \rightarrow 1$ , the frequency characteristic of an FMT subchannel is characterized by steep roll-off towards the bandedge frequencies, suggesting that per-subchannel decision-feedback equalization be performed to recover the transmitted symbols.

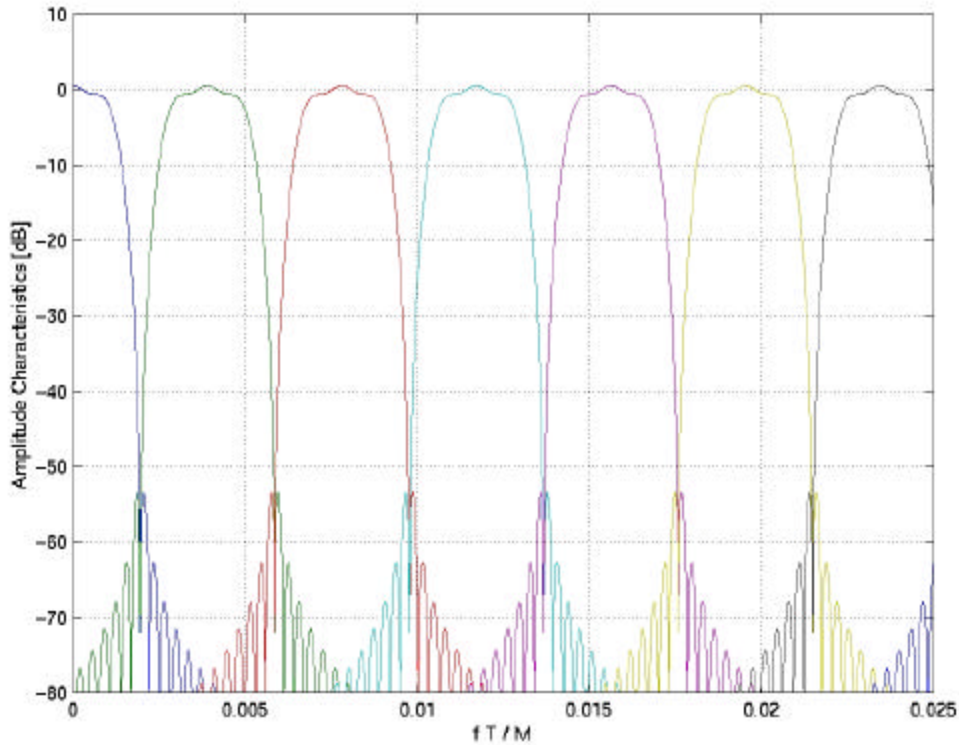


**Figure 4:** Subchannel frequency responses for  $f\chi [0, 0.025 M/T]$  in an FMT system with  $M=256$  and prototype filter designed for  $r=0.1$  and  $\uparrow=10$ .

In the second example, we employ for the prototype filter a Nyquist filter with nonzero excess bandwidth and allow noncritical sampling  $K > M$ . A square-root raised cosine filter with excess bandwidth  $\mathbf{a}$  and transfer function [6]

$$\tilde{H}_2(f_N) = \begin{cases} 1 & |f_N| \leq (1-\mathbf{a})/2 \\ \frac{1}{\sqrt{2}} \sqrt{1 - \sin \frac{\mathbf{P}}{\mathbf{a}} (|f_N| - \frac{1}{2})} & \frac{1-\mathbf{a}}{2} \leq |f_N| \leq \frac{1+\mathbf{a}}{2} \end{cases}$$

where  $f_N$  is normalized frequency, is a well-known example of a Nyquist filter. Then, for same carrier spacing as in the critically sampled case, if the symbol rate is decreased by a factor  $K/M$  a Nyquist filter with an excess bandwidth of

$$\mathbf{a} = \frac{K}{M} - 1$$

can be used while ensuring that the spectral energy of a subchannel is still entirely contained within the band of that subchannel. By letting  $K \rightarrow M$ , the penalty in bandwidth efficiency can be made vanishingly small at the price of an increase in implementation complexity since filters with increasingly sharper spectral roll-offs must then be realized.

Note that excess bandwidth modulation can also be achieved in the first example if noncritical sampling  $K > M$  is employed.

#### 4. FMT-based frequency division duplexing for VDSL

We focus in this contribution on an FMT system for VDSL that employs frequency division duplexing (FDD). In order to mitigate the effects of disturbance by self-NEXT, we assume that each of the  $M$  subchannels is used either for upstream or for downstream transmission but not both. All transmissions within the same cable binder follow the same subchannel frequency allocation. This implies a Zipper-like FDD technique. In the next section, performance and complexity issues for FMT-based FDD will be described for selected system parameters. Here we provide a discussion on the advantages of the proposed scheme by comparing it to the CAP/QAM and DMT-based techniques currently proposed for VDSL.

The following remarks can be made with respect to CAP/QAM:

- FMT modulation permits efficient implementation of a CAP/QAM scheme with more than two bands as presently proposed. Implementation efficiency stems from an all-digital generation of a multiband CAP/QAM-like signal with minimum analog filtering requirements.
- Digital filters with fairly sharp spectral roll-offs can be employed in FMT modulation, thus allowing subchannels to be placed close to each other. The guard bands needed for subchannel separation in CAP/QAM lead to a waste of useful spectrum.
- Similar to CAP/QAM systems, the receiver of an FMT system incorporates adaptive linear or decision-feedback equalization, possibly in fractionally spaced form. Although per-subchannel equalization adds to system complexity, it is very important to keep in mind that the equalizers

operate at the FMT symbol rate and not at the high transmission rate like in CAP/QAM receivers.

- Providing more than two subchannels for transmission, typically 16, 32, 64, or 128 for VDSL applications, allows bringing all advantages of a multicarrier scheme (long symbol duration, flexibility in upstream/downstream subchannel assignment, mitigation of narrowband interference, ease of meeting spectral compatibility requirements, etc.) into a CAP/QAM-like system.

The following remarks can be made with respect to DMT-based Zipper:

- DMT-Zipper requires introducing a cyclic prefix and a cyclic suffix to combat the effects of intersymbol interference introduced by the channel and to maintain signal orthogonality between subchannels in the presence of echo signals. These cyclic extensions lead to a loss in transmission efficiency. Note that to provide robustness against self-NEXT disturbance via the windowing and shaping technique the cyclic extensions must be further expanded. No cyclic extension is needed for FMT modulation due to the high level of subchannel isolation.
- Even in the case where windowing-and-shaping is used, DMT-Zipper requires that VTU-O and VTU-R transmissions be pairwise frame synchronized according to the “timing advance” technique. There are no frame synchronization requirements for FMT transmission, neither at the binder nor at a VTU-O/VTU-R pair level.
- In DMT-Zipper, windowing-and-shaping does not lead to perfect rejection of self-NEXT disturbance. For this reason, there is strong motivation to group together as much as possible the subchannels used for upstream transmission and similarly for the downstream subchannels. In FMT transmission, the subchannels can be arbitrarily assigned to upstream and downstream transmission without incurring a performance penalty due to self-NEXT.
- For FMT-based transmission a low number of subchannels can be employed as compared to DMT-based transmission. The reason for this is that FMT does not suffer from a loss of transmission efficiency (no cyclic extensions are used) as the number of subchannels is decreased, which is not the case for DMT-based transmission.

FMT modulation thus borrows features from CAP/QAM and DMT modulation techniques and offers advantages that go beyond those of each of these two modulation schemes taken individually.

## 5. Performance of FMT-based FDD for VDSL

In this section, we present simulation results to illustrate the performance achieved by FMT-based FDD systems and also compare it to that of DMT-based FDD systems. For both cases, a Zipper-like FDD scheme is assumed.

We consider the following cable transfer function, which corresponds to UTP-3 worst-case characteristics [7]:

$$C(f, \ell) = e^{-3.85 \times 10^{-6} (1+j)\sqrt{f}\ell}.$$

In this transfer function,  $f$  represents frequency in Hz,  $\ell$  the cable length in meter and constant propagation delay has been ignored.

For the results presented in this section, we consider near-end and far-end crosstalk (NEXT and FEXT, respectively) to be the main sources of interference for VDSL transmission. The power spectral densities of NEXT and FEXT signals arising from  $N$  disturbers are modeled as



$$\text{PSD}_{\text{NEXT}}(f) = \text{PSD}_{\text{disturber}}(f) \left( \frac{N}{49} \right)^{0.6} 10^{-13} f^{3/2},$$

and

$$\text{PSD}_{\text{FEXT}}(f) = \text{PSD}_{\text{disturber}}(f) |C(f, \ell)|^2 \left( \frac{N}{49} \right)^{0.6} 3 \cdot 10^{-19} \ell f^2,$$

respectively.

We measure the performance of a FMT-based system in terms of achievable bit rate for given channel characteristics. The number of bits per modulation interval that can be loaded on the  $k$ -th subchannel is given by [8]

$$b_k = \log_2 \left( \frac{\text{SNR}_k \cdot \mathbf{g}_{\text{ode}}}{\Gamma \cdot \mathbf{g}_{\text{margin}}} + 1 \right),$$

where  $\text{SNR}_k$  is the signal-to-noise ratio on the  $k$ -th subchannel,  $\mathbf{g}_{\text{ode}}$  is the coding gain,  $\Gamma$  denotes the ‘‘SNR gap’’ between the minimum SNR required for reliable transmission of  $L$  bits per modulation interval and the SNR required by  $\mathcal{L}$ -ary QAM modulation to achieve a bit error probability of  $10^{-7}$ ,  $L \gg 1$ , and  $\mathbf{g}_{\text{margin}}$  denotes the required additional margin. The achievable bit rate for downstream or upstream transmission is therefore obtained by summing the values given by  $b_k$  for downstream or upstream transmission.

Numerical results will be given for the case where the prototype filter is a linear-phase FIR filter approximation to  $\tilde{H}_1(f)$  defined in Section 3. For all cases, we use an overlap factor  $\mathbf{g} = 10$  and roll-off  $\mathbf{r} = 0.1$ . The various cases addressed will be referred to as indicated in Table 1.

Case		Nr. of subchannels (M/2)	Excess bandwidth ↳	Symbol rate
1	a	128	0 %	86.25 kHz
	b	128	6.25 %	81.18 kHz
	c	128	12.5 %	76.67 kHz
2	a	32	0 %	345 kHz
	b	32	6.25 %	324.71 kHz
	c	32	12.5 %	306.67 kHz
3	a	16	0 %	690 kHz
	b	16	6.25 %	649.41 kHz
	c	16	12.5 %	613.33 kHz

**Table 1:** Definition of the cases considered for the simulations

The power of the transmitted signal is 10 dBm. Transmission over UTP-3 cable in the presence of 49 NEXT disturbers, 49 FEXT disturbers, AWGN with power spectral density equal to  $-140$  dBm/Hz, and an echo signal negligible as compared to the other disturbances is assumed.

Achievable bit rates for symmetric transmission over the frequency band of 0 Hz to 11.04 MHz are shown in Figures 5 to 6. For all cases, per-subchannel equalization is performed by employing a Tomlinson-Harashima precoder with  $N_e^b$  taps at the transmitter and a linear equalizer with  $N_e^f$  taps

at the receiver. For the cases with zero excess bandwidth, linear symbol-spaced equalization is used, while for the nonzero excess bandwidth linear equalization with half symbol spacing is employed. The coefficients of the linear equalizer and of the precoder are equivalent to the coefficients of the forward section and of the feedback section of a MMSE DFE, respectively, and are computed assuming perfect knowledge of the subchannel characteristics. In the figures, the notation  $FMT(N_e^f, N_e^b)$  is used to indicate the number of equalizer taps used to derive system performance.

For comparison, the rates achieved by a synchronous DMT-based Zipper system with  $M = 4096$ , cyclic prefix of 150 samples, cyclic suffix of 175 samples, no time-domain equalizer and one-tap frequency equalizers are also illustrated in Figure 5a. Perfect knowledge of the overall channel characteristics has been assumed, as well as perfect synchronization of all transmissions over the 50-pair cable. Hence, the considered system achieves ideal suppression of NEXT interference.

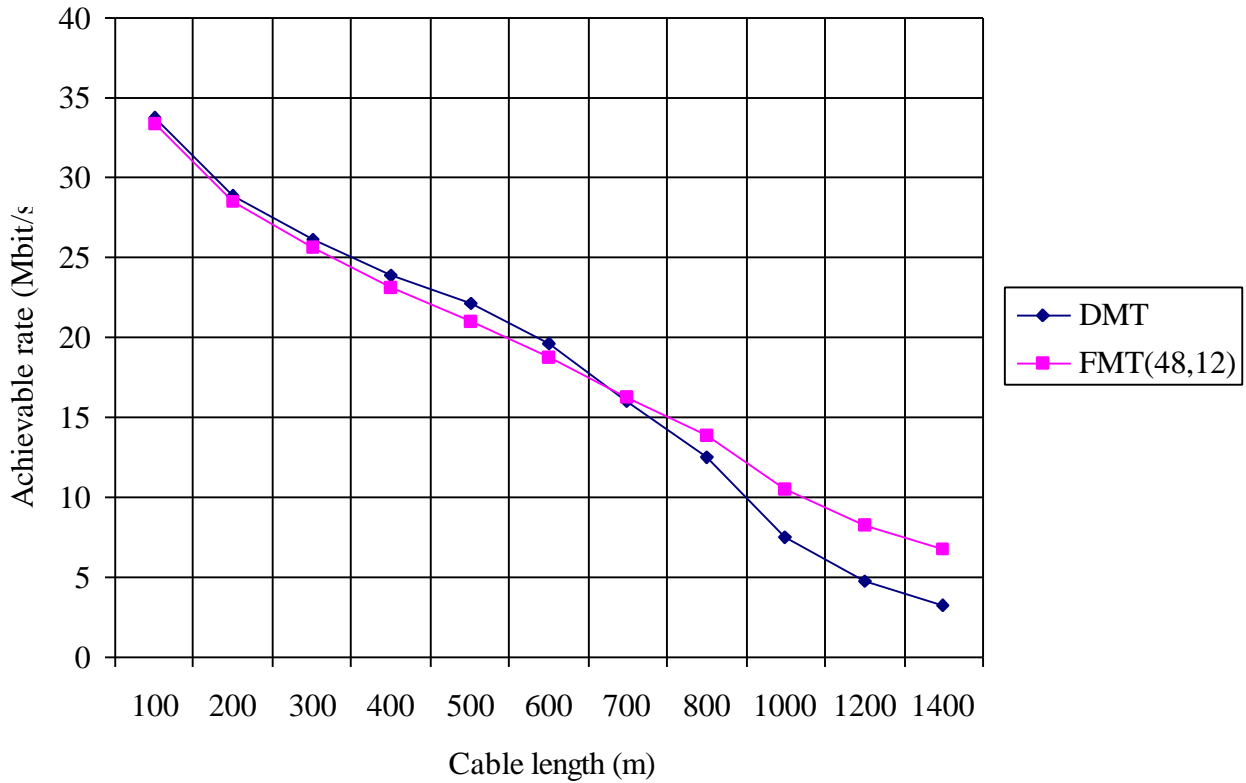


**Figure 5a:** Performance of FMT systems ( $M=256$ ) for different equalizer lengths and 0% excess bandwidth (case 1a). Performance of synchronous DMT ( $M=4096$ ) is also shown.

The results of Figure 5a indicate that FMT and DMT-based Zipper systems exhibit essentially identical performance for cable lengths up to  $\varphi 700$  m. For longer cables, where cable-dependent signal distortion becomes more significant, the FMT system allows higher data rates to be achieved due to its more powerful equalization capability. Note that in all cases the FMT-based scheme does not require any synchronization of transmissions.

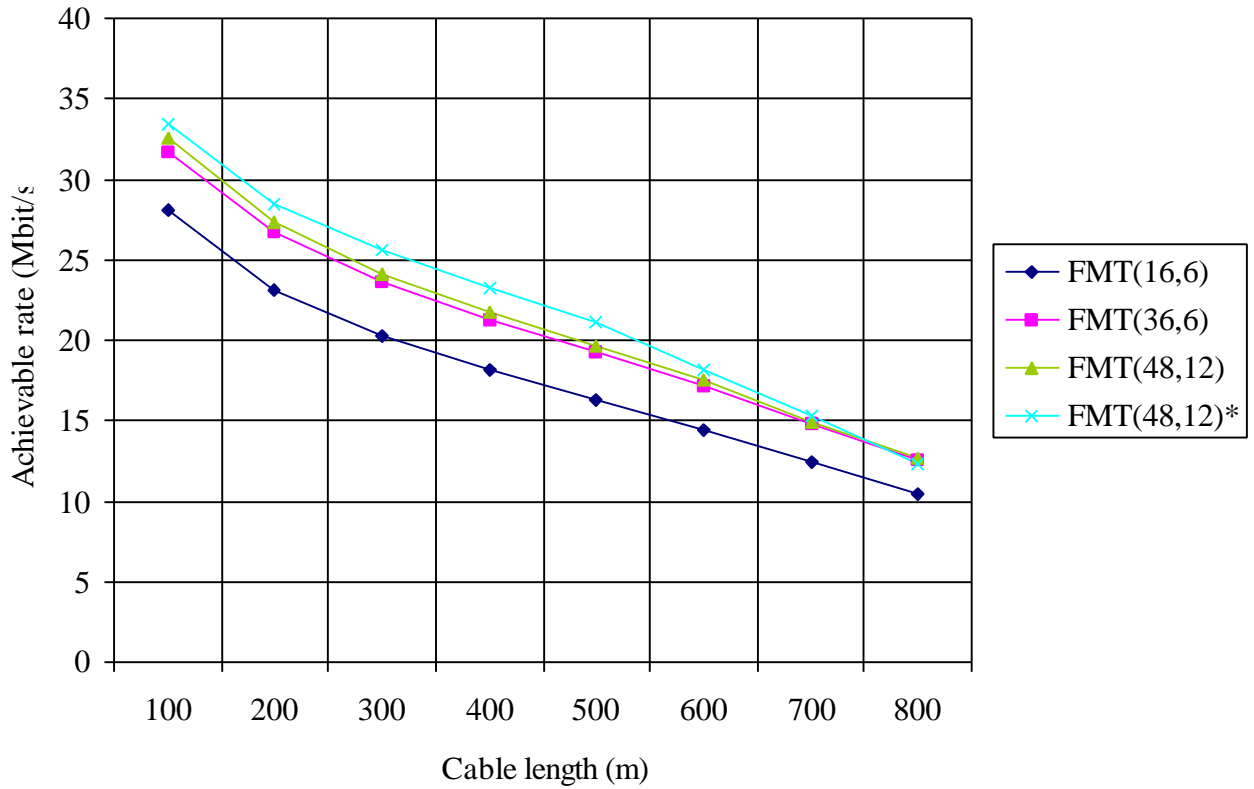


**Figure 6a:** Performance of FMT systems (M=64) for different equalizer lengths and 6.25 % excess bandwidth (case 2b). The asterisk indicates the zero excess-bandwidth case (case 2a).

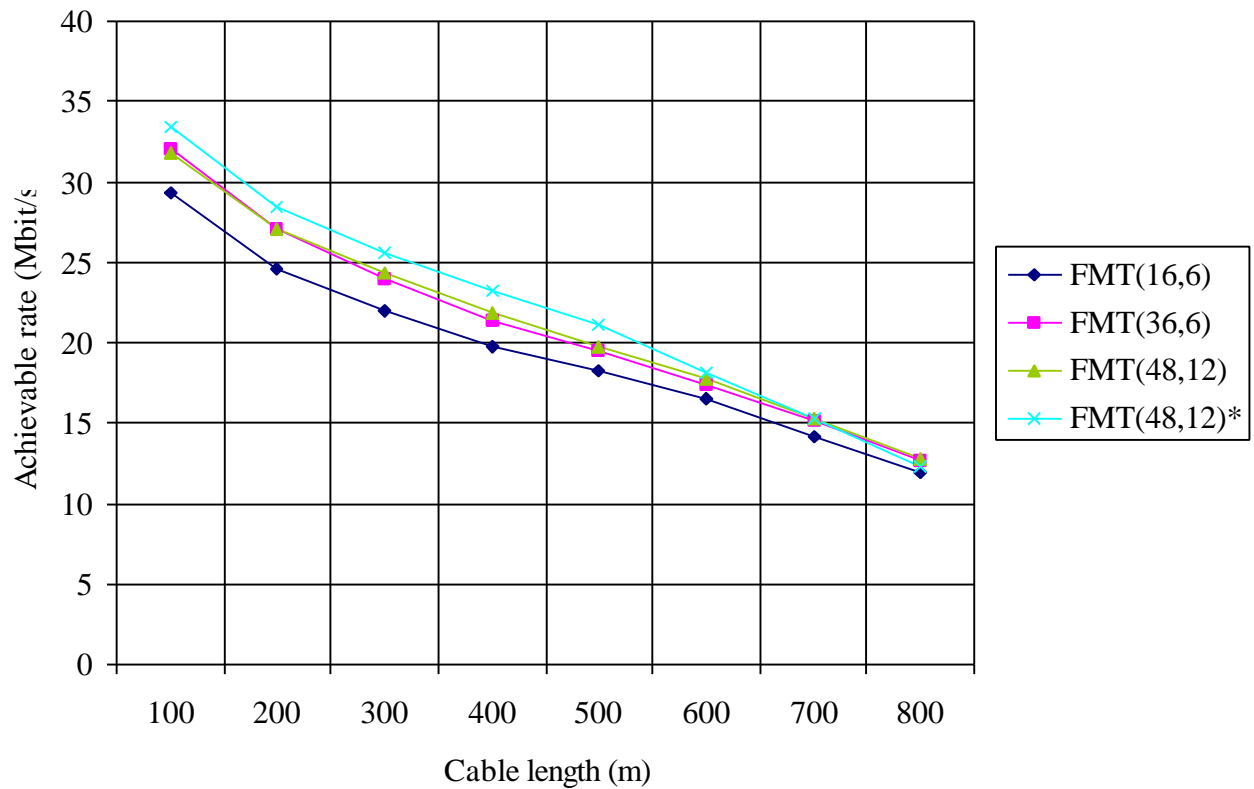


**Figure 6b:** Performance of FMT systems (M=64) for different equalizer lengths and 12.5 % excess bandwidth (case 2c). The asterisk indicates the zero excess-bandwidth case (case 2a).

## 6. Implementation complexity and latency

In this section, we first investigate the implementation complexity of FMT transmission for the different cases studied in the Section 5. Each entry in Table 2 represents, in giga ( $10^9$ ) operations (real multiply-adds) per second, the total complexity of digital filtering and fast Fourier transformation (FFT) at the transmitter and at the receiver. The number of operations for an FFT is computed as  $M \log_2 M$ , although implementations with significantly lower complexities could be used. Filter complexity is computed as the number of filter taps times the output rate, which is equivalent to the number of multiply-and-adds per second.

Case		$(N_e^f, N_e^b) = (48, 12)$	$(N_e^f, N_e^b) = (36, 6)$	$(N_e^f, N_e^b) = (16, 6)$
1	a	2.12	1.72	1.28
	b	2.10	1.70	1.26
	c	2.08	1.68	1.24
2	a	2.03	1.63	1.19
	b	2.01	1.62	1.18
	c	2.00	1.60	1.16
3	a	1.99	1.59	1.15
	b	1.97	1.58	1.13
	c	1.96	1.56	1.12

**Table 2 :** Implementation complexity in giga operations per second for the cases considered in Section 5.

Another important system design parameter is latency. The values given in Table 3 represent signal latency in  $\ell$ s from the transmit IFFT output to the receive FFT input, excluding propagation delay through the channel.

Case		$N_e^f = 48$	$N_e^f = 36$	$N_e^f = 16$
1	a	649	498	278
	b	683	535	288
	c	716	559	299
2	a	162	127	69
	b	171	134	72
	c	179	140	75
3	a	81	64	35
	b	85	67	36
	c	89	70	37

**Table 3:** Signal latency in  $\ell$ s for the cases considered in Section 5.

## 7. Conclusions

The framework of polyphase filter banks opens up a variety of possibilities to realize efficient FMT modulation systems. The objective of this contribution has been to introduce and illustrate some important aspects of these systems. The selection of the filtering elements at the transmitter as well as at the receiver represents a design tradeoff between many parameters. Further investigation is needed to determine optimum tradeoffs in connection with the VDSL system requirements.

## 8. Summary

- This contribution should be presented under G.gen.bis and is for information only.
- The described FMT modulation technique can be used for DSL transmission in general. In this contribution, it has been analyzed for VDSL transmission.

## Appendix: Polyphase representation and computationally efficient realizations

The polyphase representation [1] leads to computationally efficient implementations of multirate decimation and interpolation filters, as well as of filter banks.

Consider a filter  $H(z)$  given in  $z$ -transform notation as

$$H(z) = \sum_{n=-\infty}^{\infty} h_n z^{-n}.$$

Then for any integer  $M$ , we can decompose  $H(z)$  as:

$$H(z) = \sum_{n=-\infty}^{\infty} h_{nM} z^{-nM} + z^{-1} \sum_{n=-\infty}^{\infty} h_{nM+1} z^{-nM} + \dots + z^{-(M-1)} \sum_{n=-\infty}^{\infty} h_{nM+M-1} z^{-nM}.$$

This can be expressed as:

$$H(z) = \sum_{m=0}^{M-1} z^{-m} E^{(m)}(z^M),$$

where

$$E^{(m)}(z) = \sum_{n=-\infty}^{\infty} e_n^{(m)} z^{-n}, \quad \text{with } e_n^{(m)} = h_{nM+m}, \quad 0 \leq m \leq M-1.$$

The last equation for  $H(z)$  is called the (type 1) polyphase representation of  $H(z)$  with respect to  $M$ , and  $E^{(m)}(z)$ ,  $0 \leq m \leq M-1$ , are the polyphase components of  $H(z)$ .

We now apply the polyphase representation to show how the computationally efficient realization of Figure 3(b) can be derived from Figure 3(a) for  $K = M$ . The signal at the channel input in Figure 3(a) is given, for  $f_i = i/T$ , by

$$X_n = \sum_{i=0}^{M-1} \sum_{k=-\infty}^{\infty} A_k^{(i)} h_{n-kM} e^{j2\pi i n/M},$$

which can be rearranged as

$$X_n = \sum_{k=-\infty}^{\infty} h_{n-kM} \sum_{i=0}^{M-1} A_k^{(i)} e^{j2\pi i n/M}.$$

A change of notation  $n = \ell M + m$  allows us to introduce the polyphase components of  $h_n$ . With the notations  $x_{\ell M+m} = x_\ell^{(m)}$  and  $h_{\ell M+m} = h_\ell^{(m)}$ ,  $m = 0, 1, \dots, M-1$ , we obtain:

$$x_\ell^{(m)} = \sum_{k=-\infty}^{\infty} h_{\ell-k}^{(m)} \sum_{i=0}^{M-1} A_k^{(i)} e^{j2\pi i m/M} = \sum_{k=-\infty}^{\infty} h_{\ell-k}^{(m)} a_k^{(m)},$$

where  $a_k^{(m)}$ ,  $0 \leq m \leq M-1$ , is the inverse discrete Fourier transform (IDFT) of  $A_k^{(i)}$ ,  $0 \leq i \leq M-1$ .

## References

- [1] M. Bellanger, G. Bonnerot, and M. Coudreuse, "Digital filtering by polyphase network: application to sample-rate alteration and filter banks," *IEEE Trans. Acoust., Speech, Signal Processing*, vol. ASSP-24, No. 2, pp. 109-114, Apr. 1976.
- [2] P.P. Vaidyanathan, *Multirate systems and filter banks*. Englewood Cliffs, NJ: Prentice-Hall, 1992.
- [3] S.D. Sandberg and M.A. Tzannes, "Overlapped discrete multitone modulation for high speed copper wire communications," *IEEE J. Select. Areas Commun.*, vol. 13, No. 9, pp. 1571-1585, Dec. 1995.
- [4] M.V. Eyuboglu and G.D. Forney, "Trellis precoding: Combined coding, precoding and shaping for intersymbol interference channels," *IEEE Trans. Inform. Theory*, vol. 38, pp. 301-314, Mar. 1992.
- [5] M. Isaksson, P. Deutgen, F. Sjöberg, S.K. Wilson, P. Ödling, and P.O. Börjesson, "Zipper – A flexible duplex method for VDSL," Proc. 1998 IEEE Int. Conf. on Communications, paper S29-7, Atlanta, GA, June 1998.
- [6] G.H. Im and J.J. Werner, "Bandwidth-efficient digital transmission over unshielded twisted-pair wiring," *IEEE J. Select. Areas Commun.*, vol. 13, No. 9, pp. 1643-1655, Dec. 1995.
- [7] "Commercial Building Telecommunications Cabling Standard," EIA-TIA Standard PN 2840, EIA/TIA 568-A, Mar. 1994.
- [8] J.M. Cioffi, "Asymmetrical digital subscriber lines," in *The Communications Handbook*, J.D. Gibson (Ed.), CRC Press Inc., pp. 450-479, 1997.